



Light and heavy ferritin chain expression in the liver and kidneys of Wistar rats: aging, sex differences, and impact of gonadectomy

Mirela Pavić Vulinović¹, Petra Turčić², Vedran Micek³, and Marija Ljubojević³

¹ University of Zagreb Faculty of Veterinary Medicine, Department of Anatomy, Histology and Embryology, Zagreb, Croatia

² University of Zagreb Faculty of Pharmacy and Biochemistry, Department of Pharmacology, Zagreb, Croatia

³ Institute for Medical Research and Occupational Health, Zagreb, Croatia

[Received in December 2021; Similarity Check in December 2021; Accepted in March 2022]

Ferritin is the main intracellular storage of iron. Animal studies show that female liver and kidney express more ferritin and accumulate more iron than male. However, no study so far has investigated sex and age differences in light (FtL) and heavy (FtH) ferritin chain expression. To address this, we relied on specific antibodies and immunochemical methods to analyse the expression of both ferritin chains in the liver and kidney of 3-month and 2-year-old male and female Wistar rats. To see how sex hormones may affect expression we also studied adult animals gonadectomised at the age of 10 weeks. FtL and FtH were more expressed in both organs of female rats, while gonadectomy increased the expression in males and decreased it in females, which suggests that it is stimulated by female and inhibited by male steroid hormones. Normal kidney ferritin distribution and change with aging warrant more attention in studies of (patho) physiological and toxicological processes.

KEY WORDS: ferritin nanocage; hepatocytes; immunofluorescence; intercalated cells, iron metabolism; *macula densa*; nephron; steroid hormones; western blot

Structurally, the mammalian ferritin complex is a hollow protein sphere or a nanocage composed of 24 subunits from two protein chains, light (FtL: 183 amino acids) and heavy (FtH: 182 amino acids). A ferritin nanocage can accommodate about 4500 Fe(III) atoms, mostly in the form of bioavailable mineral ferrihydrite, and a significant amount is present in the liver, heart, spleen, and kidneys (1–3).

Several genetic studies reported a more vital role of FtH than of FtL, as its silencing causes early embryonic death, whereas mice without FtL survive. Although both chains are structured as intracellular nanocages, FtH also promotes ferroxidase activity, which mediates oxidation of the ferrous [Fe (II)] into a less reactive ferric [Fe (III)] ion (1–8).

Previous sex and aging studies have shown that ferritin expression reflects iron accumulation and that ferritin is higher in female than male and in older than younger experimental animals (9–18). These sex and age differences may be owed to the liver hormone hepcidin as the main regulator of systemic iron availability. Hepcidin expression is higher in female rats and depends on steroid hormones (7, 18).

At the moment, however, we do not know how sex and age differences affect the expression of either ferritin chain in the kidney

and liver and whether they affect them differently, as, to the best of our knowledge, such studies have not yet been carried out (9, 10). The aim of this study was, therefore, to determine liver and kidney expression of both ferritin chains in adult and old male and female animals and to establish the effect of hormone loss (through gonadectomy of adult animals) on their individual expression.

MATERIALS AND METHODS

Animals and treatment

Sex and age differences were studied in three-month and two-year-old male and female Wistar rats from the colony bred at the Institute for Medical Research and Occupational Health, Zagreb, Croatia. Animals had free access to tap water and standard pelleted food (4RF21, Mucedola, Settimo Milanese, Italy) and were treated in accordance with the Directive 2010/63/EU (19) on the protection of animals used for scientific experiments. The gonadectomised group consisted of four 10-week old males castrated via scrotal route and four females ovariectomised via dorsal route two weeks before sacrifice. For control we used four respective male and female

sham-gonadectomised animals, which underwent operation without removing their reproductive organs (20). The sacrifice and operations were performed under general anaesthesia with intraperitoneal ketamine (80 mg/kg body mass) and xylazine (12 mg/kg body mass) (Chassot AG, Bern, Switzerland). The studies were approved by the Institute's Ethics Committee and by the Croatian Ministry of Agriculture under the AGEMETAR project.

Antibodies

Monoclonal antibodies against target proteins FtL (sc-390558, D-1) and FtH (sc-376594, B-12) or housekeeping proteins alpha-tubulin (sc-23948, aT), beta-actin (sc-47773, bA), and glyceraldehyde-3-phosphate dehydrogenase (sc-365062, GAPDH, G) were obtained from Santa Cruz Biotechnology (Dallas, TX, USA). Secondary antibodies were bought from Jackson ImmunoResearch Laboratories (West Grove, PA, USA). The alkaline phosphatase-labelled goat anti-mouse IgG (GAMAP; Cat. No. 115-056-068) was used for western blotting and CY3-labeled donkey anti-mouse IgG (DAMCY3; Cat. No. 715-165-151) for immunohistochemical analysis.

Sample preparation and western blotting

We removed part of the liver and kidney from each sacrificed animal and dissected it manually to prepare 10 % tissue homogenates in an ice cold pH 7.4 buffer containing 300 mmol/L mannitol, 5 mmol/L EGTA, 12 mmol/L Tris/HCl, and protease inhibitors (SIGMAFAST™, Cat. No. S8830, Sigma-Aldrich, St. Louis, MO, USA) using a Powergen 125 homogeniser (Fisher Scientific, Clifton, NJ, USA). These crude homogenates were centrifuged at 5,000 *g* for 15 min, pellets discarded, and supernatants used to identify ferritin chains with western blotting. Protein concentrations were measured with the dye-binding assay and homogenates frozen at -20 °C until further use (20, 21).

For sodium dodecyl sulphate-polyacrylamide gel electrophoresis (SDS-PAGE), liver or kidney tissue homogenates were mixed with Laemmli sample buffer (20, 21) with or without 2-mercaptoethanol and denatured at various temperatures. Proteins (40 or 60 µg per lane) were separated with 18 % or 20 % SDS-PAGE gels using a Mini-PROTEAN 3 system and then wet-transferred using Mini Trans-Blot Electrophoretic Transfer Cell (both from Bio-Rad Laboratories, Hercules, CA, USA) to the poly(vinylidene fluoride) (PVDF) membrane (Immobilon®, Millipore, Bedford, MA, USA). Some PVDF membranes were stained with Coomassie blue (CBS) (Figure 1B) to check that we had the same load of proteins for all samples and the rest were immediately incubated with 1 % glutaraldehyde (GA) for 30 min as described elsewhere in detail (20, 21) to fixate small proteins on the membrane. We did this because FtL (antibody D-1) did not stain without GA fixation, whereas FtH (antibody B-12) staining was not affected by GA, which indicates different hydrophilic properties of the two subunits (data not shown).

PVDF membranes were incubated with target and housekeeping antibodies diluted in blotting milk – D-1 at the 1:1000 ratio, and B-12, aT, bA, and GAPDH at the 1:500 ratio. As we could not detect housekeeping proteins in some liver samples with colourimetry because of high gel density, we relied on the nonspecific band (NB) stained with secondary antibodies, as it appeared uniform below the ferritin protein band (Figures 1B, 4A, and 5A). After colourimetric-detection, we evaluated protein band densities relative to the density of the strongest protein band in control samples (1 arbitrary unit) using the open source ImageJ program (US National Institutes of Health, MA, USA).

Tissue fixation and immunohistochemistry

As described in detail in our previous work (20, 21), liver and kidneys were perfused with 4 % paraformaldehyde (PFA) *in vivo* via the left heart ventricle for 5 min while the animals were under anaesthesia. Liver and kidneys were then removed, sliced in 1–2 mm thick slices, kept in 4 % PFA at 4 °C overnight, thoroughly washed in phosphate-buffered saline containing 0.02 % NaN₃ (PBS), and refrigerated in PBS until use.

The slices were soaked overnight in 30 % sucrose (in PBS), embedded in an optimal cutting temperature medium (Tissue-Tek, Sakura, Japan), frozen to -25 °C, cut to 4 µm thick cryosections with a Leica CM 1850 cryotome (Leica instruments, Nussloch, Germany), and placed on Superfrost/Plus microscope slides (Fischer Scientific, Pittsburgh, PA, USA). For immunostaining we followed an optimised antigen retrieval procedure for both target antibodies described in detail elsewhere (20, 21). Immunohistochemical staining was examined under an Opton III RS fluorescence microscope (Opton Feintechnik, Oberkochen, Germany) and images captured and processed with a Spot RT Slider camera and software (Diagnostic Instruments, Sterling Heights, MI, USA). We then used Adobe Photoshop 6.0 (Adobe, San Jose, CA, USA) to obtain black and white images, label them, and arrange in panels.

Data presentation and statistical analysis

Immunohistochemical and western blot data were obtained from four animals per experimental group. Group means ± standard errors of the mean (SEM) were compared with the *t*-test and the level of significance was set to *p*<0.05.

RESULTS AND DISCUSSION

Considering previous research of age and sex differences in ferritin expression (9–18), our study has confirmed its dependence on age, sex, and steroid hormones for both chains in the liver and kidney of 3-month and 2-year-old male and female Wistar rats.

Immunochemical findings in the liver are given in Figure 1. Figure 2 shows kidney panels with parallel ferritin staining in the female kidney based on consecutive cryosections. Detailed

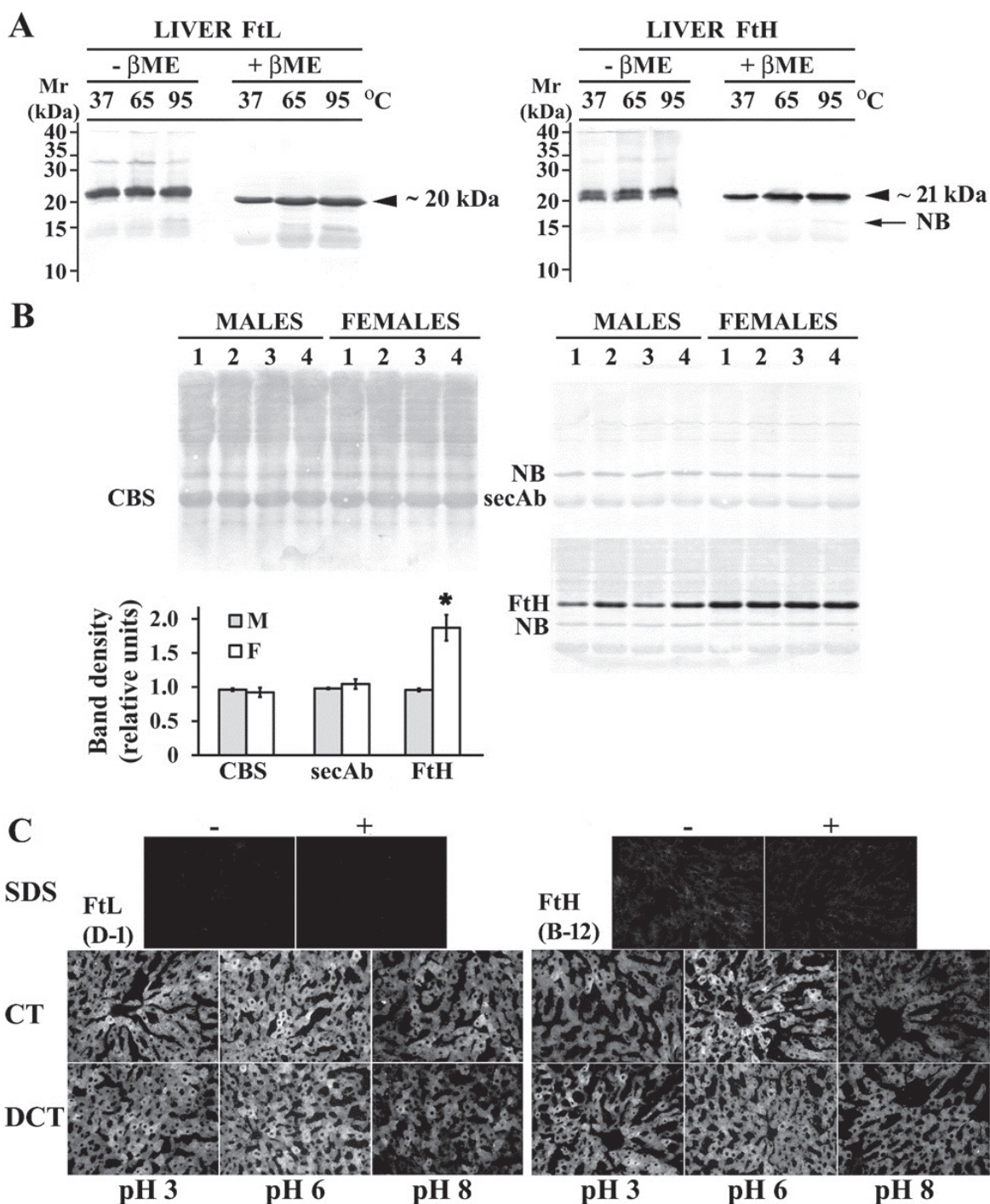


Figure 1 Liver ferritin immunocytochemistry conditions during procedure optimisation. (A) Sample preparation for Western blotting in reducing and non-reducing conditions at three temperatures that all yielded a strong and sharp protein band of 20 kDa for FtL and 21 kDa for FtH; (B) Western blotting for protein load – livers of 3-month-old male and female stained with Coomassie blue staining (CBS). PVDF membrane was incubated only with secondary antibody (secAb) followed by FtH antibody reincubation. Densitometric result between CBS samples and secondary antibody nonspecific band (NB) staining did not show difference vs protein band after FtH staining; (C) Antigen retrieval conditions for immunofluorescent staining for both ferritin antibodies. No staining was observed either without retrieval or with sodium dodecyl sulphate (SDS). Microwave cooking in citrate buffer (CT) with different pH gave best results for both ferritin antibodies at pH 6. Sham deparaffinisation with organic solutions and alcohol prior to cooking in citrate buffer (DCT) did not increase staining intensity

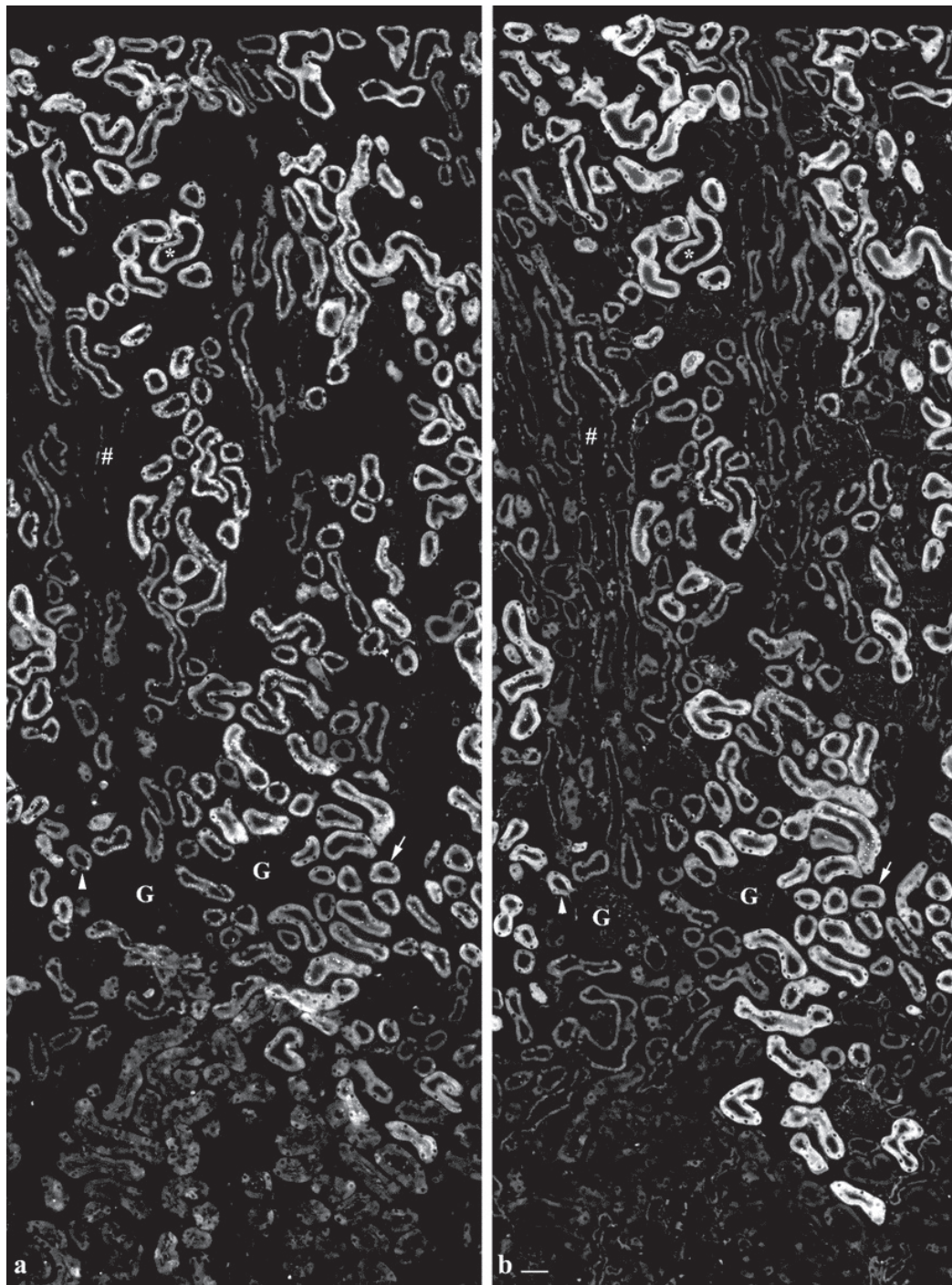


Figure 2 Kidney panels with parallel ferritin staining in consecutive cryosections of female kidney. Immunofluorescence of FtL (a) and FtH (b) shows stronger staining in epithelial cells of proximal tubules throughout the cortex and much weaker and mosaic staining in the outer stripe of kidney zones. Proximal tubules showed homogenous intracellular staining, whereas some S1 and S2 segments showed relatively dotted and faint (a, FtL) to strong (b, FtH) staining. Arrowheads on both panels show S1 segment of the proximal tubule (a, b) leaving juxtamedullar glomeruli (G). On the b panel S2 segments show homogenous and strong staining (arrow in G proximity). Faint (a,b) and mosaic staining (a) was observed in S3 segments (bottom of panels below G). Many proximal tubules contained ferritin-positive vesicles in the cells and in the lumen (asterisk in the S2 segment). This was found for both chains in the same cells/tubules of consecutive cryosections (a and b panels). However, FtH was more prominently stained in structures such as intercalated cells in the collecting duct (ladder) and weakly in the thick ascending limb of Henley (tubule to the left above the ladder). Bar=50 μ m

distribution of ferritin chain expression in the kidneys is shown in Figure 3.

Figures 4 and 5 show immunochemistry findings of light and heavy ferritin chains in the liver and Figures 6 and 7 in the kidney. The effect of gonadectomy on both ferritin chains in the liver is detailed in Figure 8 and in the kidney in Figure 9.

We have confirmed sex and age-dependent expression of both ferritin chains in the liver and kidneys (Figures 4–7), as female rats had more than two times as high expression as males. Similar findings in the liver and kidney were reported for iron accumulation (11–14, 20, 22).

We have also demonstrated that the expression of both ferritin chains depends on sex hormones, as it was higher after castration and lower after ovariectomy (Figures 8 and 9), which is in line with studies of iron accumulation conducted a few decades earlier (9, 10, 14) and our more recent report of iron turnover after castration and ovariectomy (20).

Even though both ferritin chains are responsive to sex hormones, they do not have oestrogen or androgen response elements in their promoters. This suggests that iron regulates their expression through iron response proteins (IRP) and elements (IRE) in conformations of mRNA (1–7).

Some details we observed in the staining of both ferritin chains in three-month and two-year-old kidneys warrant more rigorous investigation that would include colocalisation analysis of specific

proteins to confirm the presence of both in same cellular locations, as indicated by unexpected localisation of ferritin chains in intercalated cells and *macula densa* in our histological findings. Intercalated cells are involved in sequestering iron through complex neutrophil gelatinase-associated lipocalin/receptor-mediated endocytosis during inflammation (23), whereas *macula densa* cells seem to involve the expression of hypoxia sensors and erythropoietin, which may explain the strong staining of both ferritin chains ready to release iron for enzymes needed in erythropoietin expression (24).

The role of iron in kidney diseases has recently been emphasised, and more precise localisation of ferritin throughout the kidney may tell us more about its functions in (pato)physiology (5, 25–28). However, protein expression in organs detected by western blotting in our study has yet to be confirmed by *in situ* distribution in order to reveal a more precise expression pattern.

Our findings have shown strong ferritin staining of interstitial cells irregularly present in all kidney zones. We assume that it could be associated with macrophages (Figures 6 and 7, c and d), as macrophages have recently been recognised as a new source of serum ferritin (25, 28). This could be relevant for our positive findings of ferritin in aged rats.

Another interesting finding in our study is intracellular abundance of ferritin-positive vesicles, which may reflect ferritin/iron lysosomal turnover. Lysosomal iron may be protected with

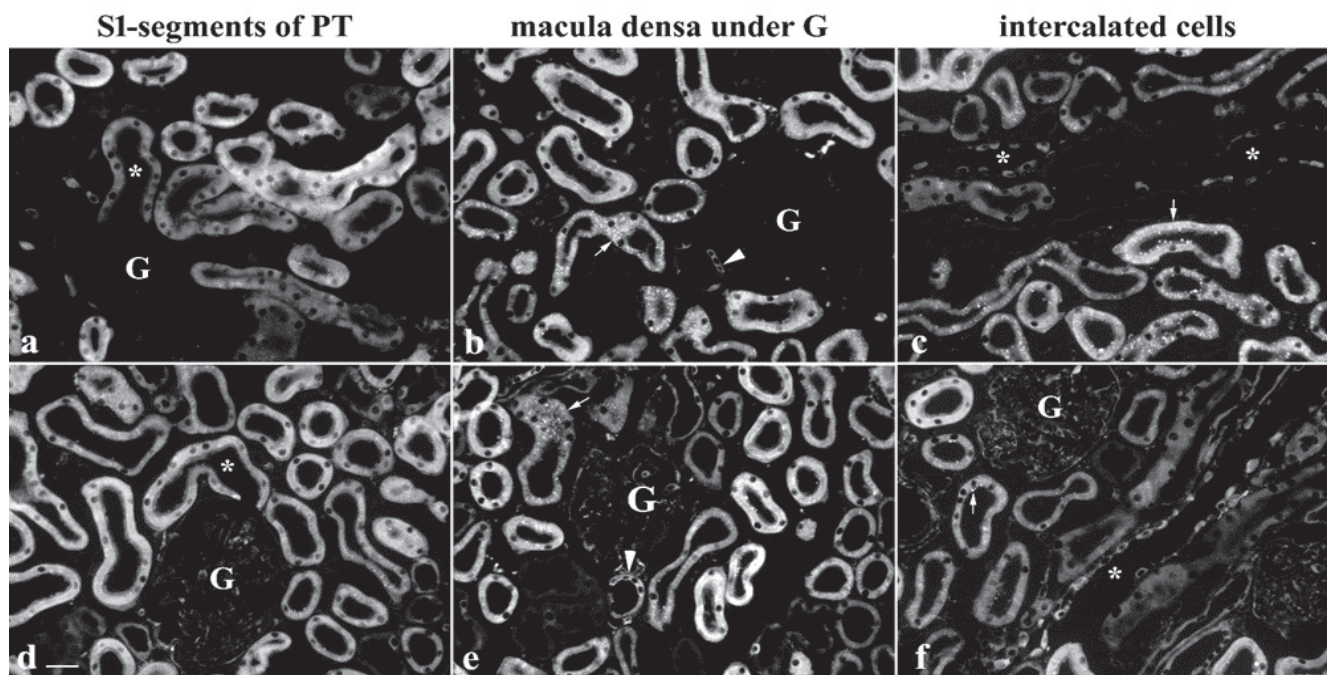
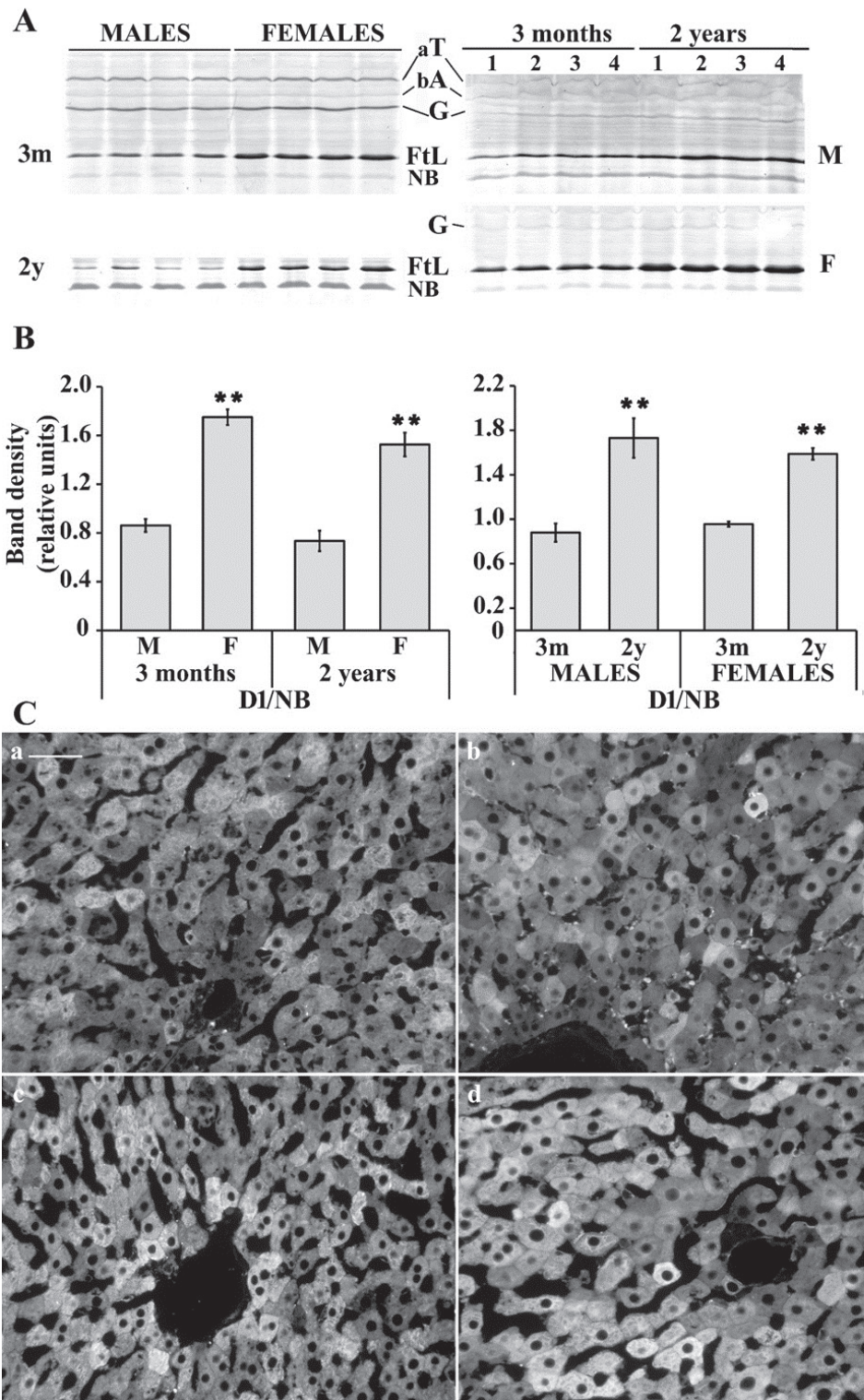
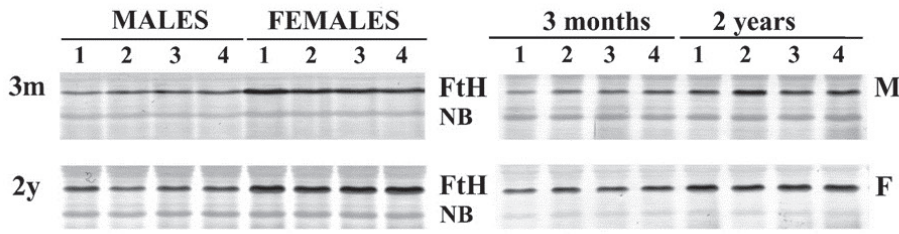


Figure 3 Details of ferritin chain expression in the kidneys. Panel a, b, and c show FtL and panels d, e, and f FtH staining in specific nephron segments. Intracellular staining was mostly homogenous in epithelial cells of the proximal tubule (PT). Staining in the S1 segment leaving glomeruli (G) was relatively faint for FtL (a) and stronger for FtH (d) (asterisk in the S1 segment of PT leaving G). Ferritin-positive were specific structures of *macula densa* with both antibodies (arrowhead in b, e below G). Intracellular vesicles can be seen in all PT tubules (arrow in b and e) and in the PT lumen (arrow in c and f). Both ferritin chains were positive in intercalated cells of the collecting duct (asterisk in c, f). Panels d, e, and f show some positive FtH staining in glomeruli, possibly in the podocytes, mesangial cells, and/or parietal layer. This was not prominent with FtL (G in a, b). Bar=20 μ m

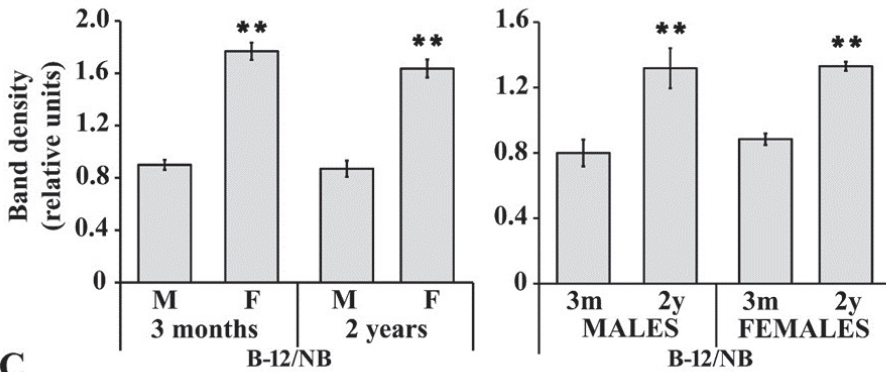
Figure 4 Immunocytochemistry of the light ferritin chain in the liver. Western blotting with D-1 antibody against FtL (A) followed by densitometric evaluation (B) of the protein bands labeled in liver tissue homogenates. FtL immunostaining in cryosections of the liver tissues of three-month (3m) and two-year (2y) old male (M) and female (F) rats (C). The strong protein band of ~ 20 kDa represents the FtL chain and was used for densitometric evaluation in relation to NB (A). Each band represents FtL protein expression in tissue homogenates from individual animals. Higher expression of FtL is visible in female rats regardless of age and in 2-year-old male and female animals. Additional protein bands are from alpha-tubulin (aT), beta-actin (bA), and GAPDH (G) as unused housekeeping proteins. Densitometric evaluation of protein bands (B) is shown by bars, each representing mean ± SEM of band density of four animals per group. Statistics: vs respective M or 3-month-old animals, **P<0.01. Immunohistochemical images of FtL in liver tissue cryosections (C) show similar findings in 3m (a, b) and 2y (c, d) old M (a, c) and F (b, d) rats. Intracellular staining is stronger in 3m old F vs 3m old M (a, b) and 2y old F vs 2y old M (c, d), 2y old M vs 3m old M (a, c), and 2y old F (b, d) vs 3m old F. Bar=30 μm



A



B



C

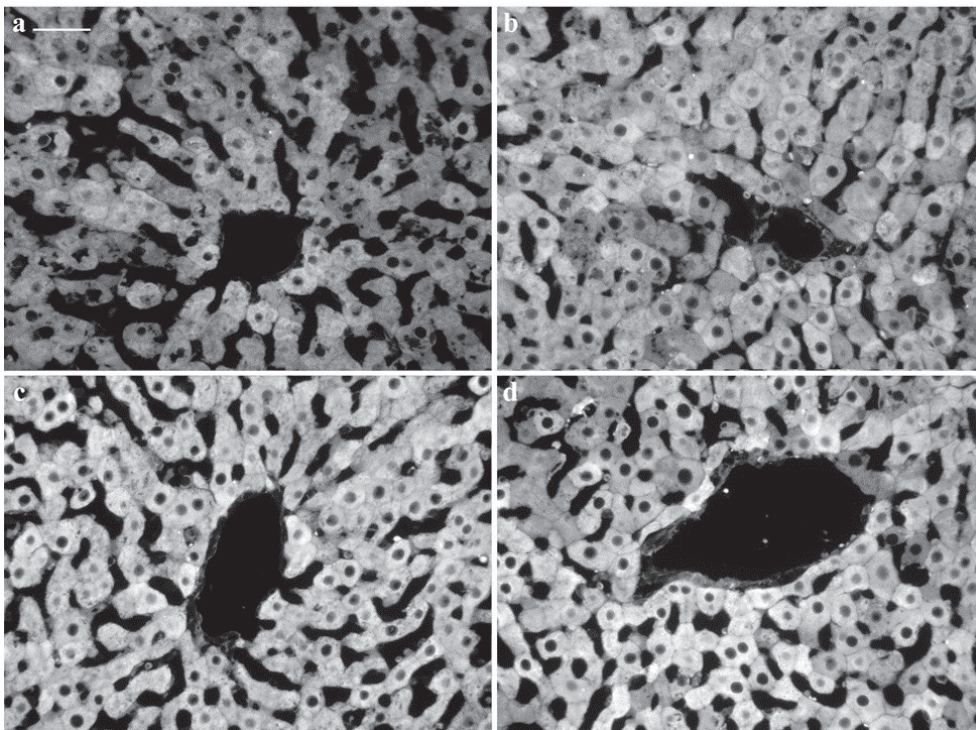
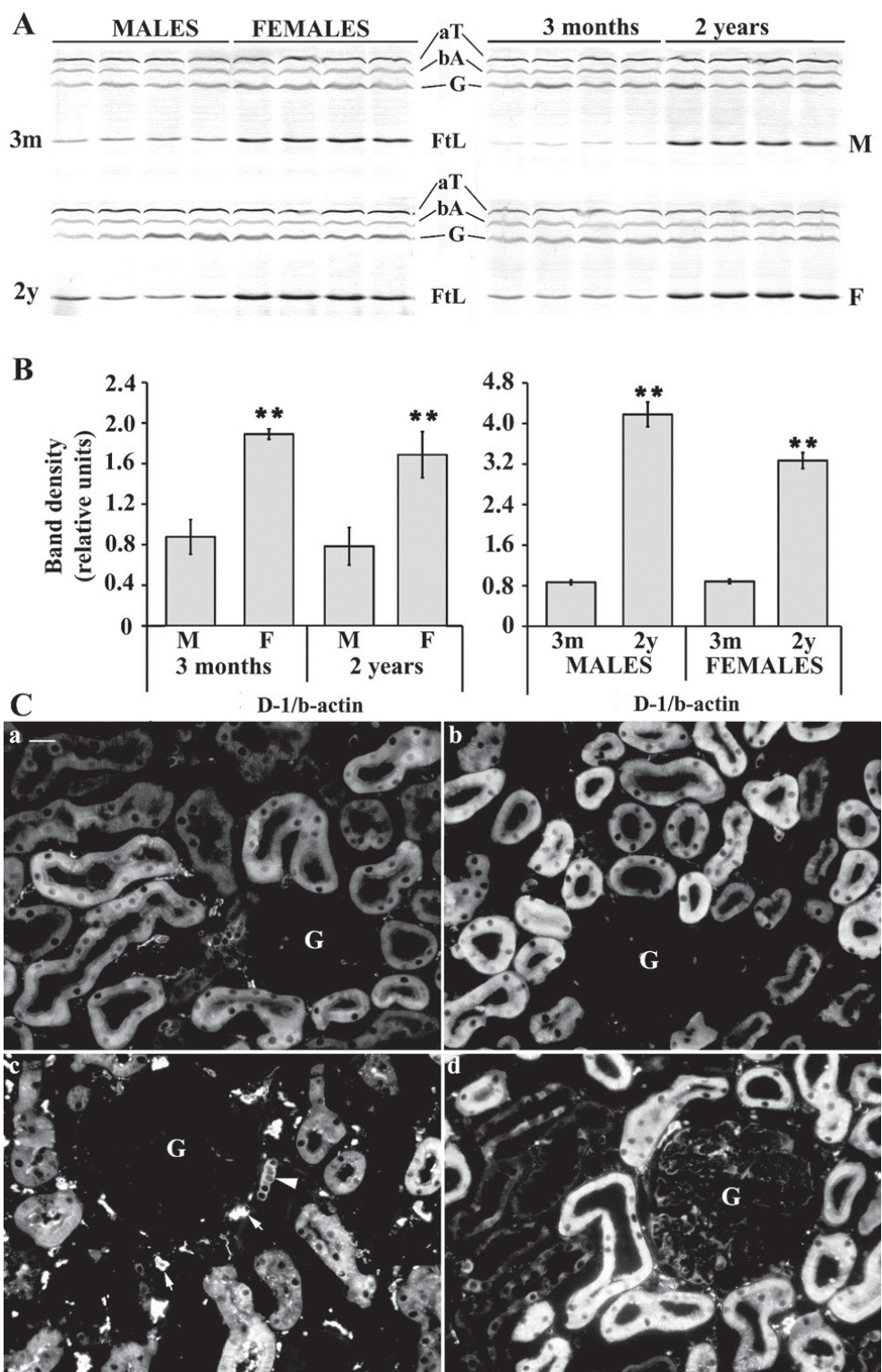


Figure 5 Immunocytochemistry of the heavy ferritin chain in the liver. Western blotting with B-12 antibody against FtH (A) and densitometric evaluation (B) of the protein bands. FtH immunostaining in cryosections of the liver tissues of three-month (3m) and two-year (2y) old male (M) and female (F) rats (C). The strong protein band of ~21 kDa represents the FtH and was used for densitometric evaluation in relation to NB. Each band represents FtH protein expression in tissue homogenates from individual animals. Higher expression of FtH is visible in female rats regardless of age and in 2-year-old male and female animals in M and F. Densitometric evaluation of the protein bands (B) is shown by bars, each representing mean \pm SEM of band density of four animals per group. Statistics: vs respective males or 3-month-old animals, **P < 0.01. Immunohistochemical images of FtH in liver tissue cryosections (C) show similar findings in 3m (a, b) and 2y (c, d) old M (a, c) and F (b, d) rats. Intracellular staining is stronger in 3m old F vs 3m old M (a, b) and in 2y old F vs 2y old M (c, d) and in 2y old M vs 3m old M (a, c) and in 2y old F vs 3m old F (b, d). Bar=30 μ m

Figure 6 Immunocytochemistry of the light ferritin chain in the kidney. Western blotting with D-1 antibody against FtL (A) followed by densitometric evaluation (B) of the protein bands labeled in kidney tissue homogenates. FtL immunostaining in cryosections of the kidney tissues of three-month (3m) and two-year (2y) old male (M) and female (F) rats (C). The strong protein band represents FtL and was used for densitometric evaluation in relation to beta-actin (bA). Each band represents FtL protein expression in tissue homogenates from individual animals. Higher expression of FtL is visible in female rats regardless of age and in 2-year-old male and female animals. Additional protein bands are from alpha-tubulin (aT), beta-actin (bA), and GAPDH (G) as housekeeping proteins. Densitometric evaluation of protein bands (B) is shown by bars, each representing mean \pm SEM of band density of four animals per group. Statistics: vs respective M or 3m old animals, $**P < 0.01$. Immunohistochemical images of FtL in kidney tissue cryosections (C) show similar findings in 3m (a, b) and 2y (c, d) old M (a, c) and F (b, d) rats. Intracellular staining is stronger in 3m old F vs 3m old M (a, b), 2y old F vs 2y old M (c, d), 2y old M (a, c) vs 3m old M, and 2y old F (b, d) vs 3m old F. Glomeruli (G) are marked on panel (C) and arrowhead in c marks *macula densa*, whereas arrows mark positive interstitial staining, probably macrophages. Bar=20 μ m



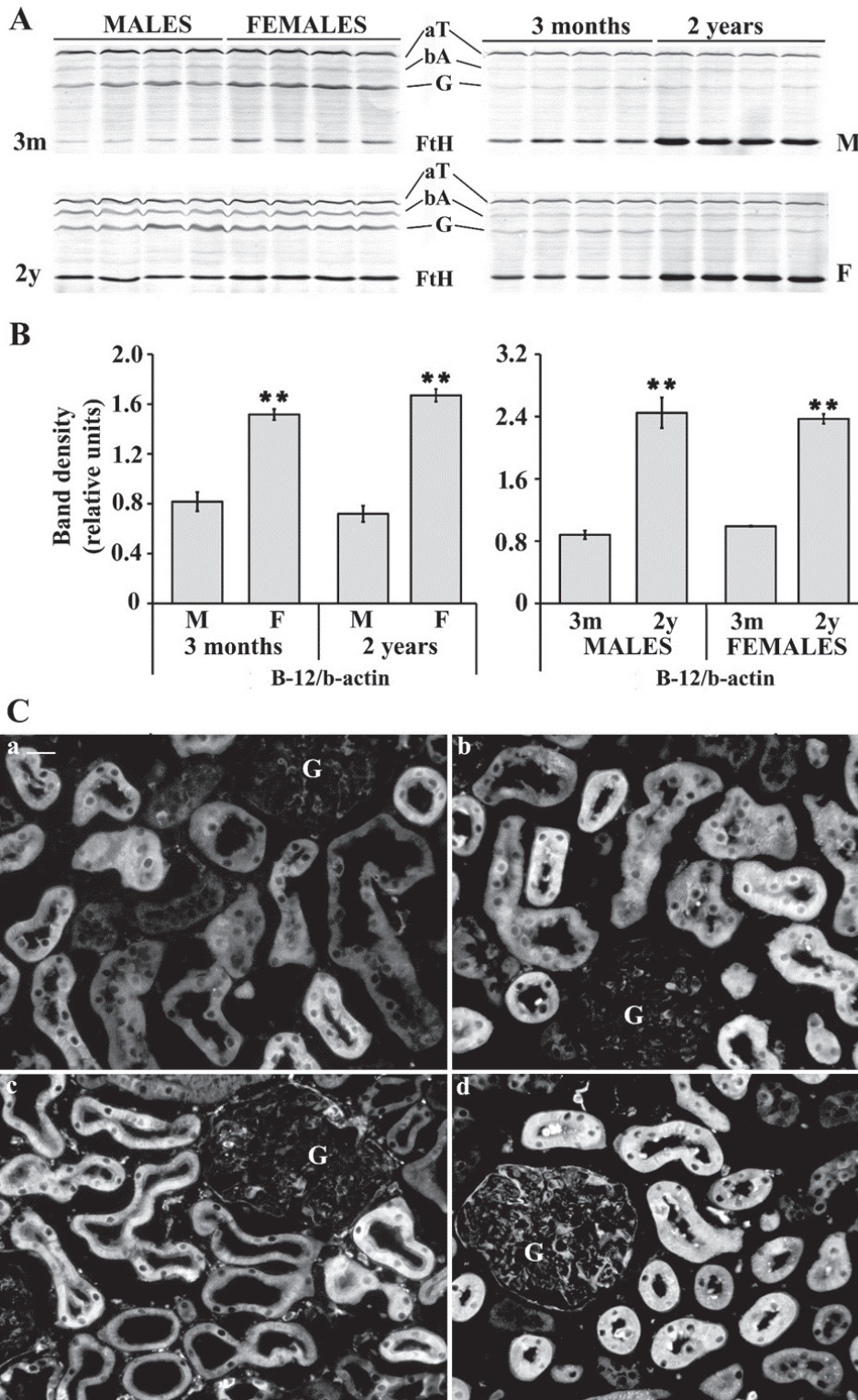


Figure 7 Immunocytochemistry of the heavy ferritin chain in the kidney. Western blotting with B-12 antibody against FtH (A), and densitometric evaluation (B) of the protein bands. FtH immunostaining in cryosections of the kidney tissue of three-month (3m) and two-year (2y) old male (M) and female (F) (C). The strong protein represents FtH and was used for densitometric evaluation in relation to beta-actin (bA) (A). Higher expression of FtH is visible in female rats regardless of age and in 2-year-old male and female animals. Each band represents FtH protein expression in tissue homogenates from individual animals. Densitometric evaluation of protein bands (B) is shown by bars, each bar representing mean \pm SEM of band density of four animals per group. Statistics: vs respective M or 3m old animals, **P < 0.01. Immunohistochemical images of FtH in kidney tissue cryosections (C) show similar findings in 3m (a, b) and 2y (c, d) old M (a, c) and F (b, d) rats. Intracellular staining is stronger in 3m old F vs 3m old M (a, b), 2y old F vs 2y old M (c, d), 2y old M vs 3m old M (a, c), and 2y old F vs 3m old F (b, d). Glomeruli (G) are marked on panel (C) and in c (2y M) and d (2y F) and are better stained in 3m M and F (a, b) (possibly present in podocytes, mesangial cells or/and parietal layer). Bar=20 μ m

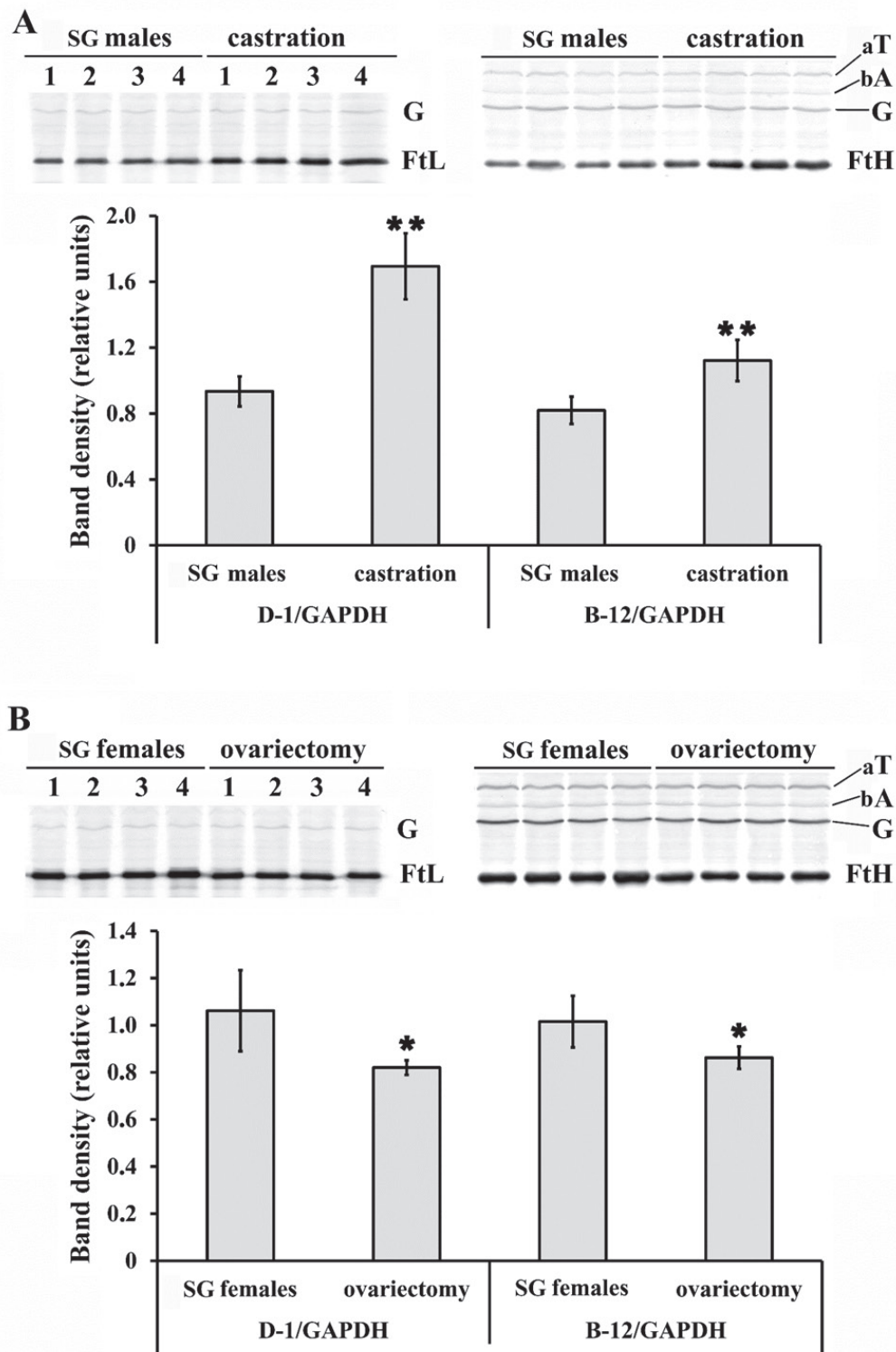


Figure 8 Effect of gonadectomy on both ferritin chain expression in the liver. Expression of FtL and FtH protein (A, B) in the liver by western blotting. Each band represents FtL or FtH expression in the tissue of individual animals. Additional protein bands are from alpha-tubulin (aT), beta-actin (bA), and GAPDH (G). Each bar represents mean \pm SEM of band density from four animals per group. Data were analysed with the *t*-test. Ovariectomy statistically decreased the expression of both ferritin chains and castration increased their expression. Statistics: sham-gonadectomised (SG) vs castrated males ** $P < 0.01$ (A); SG vs ovariectomised females * $P < 0.05$ (B)

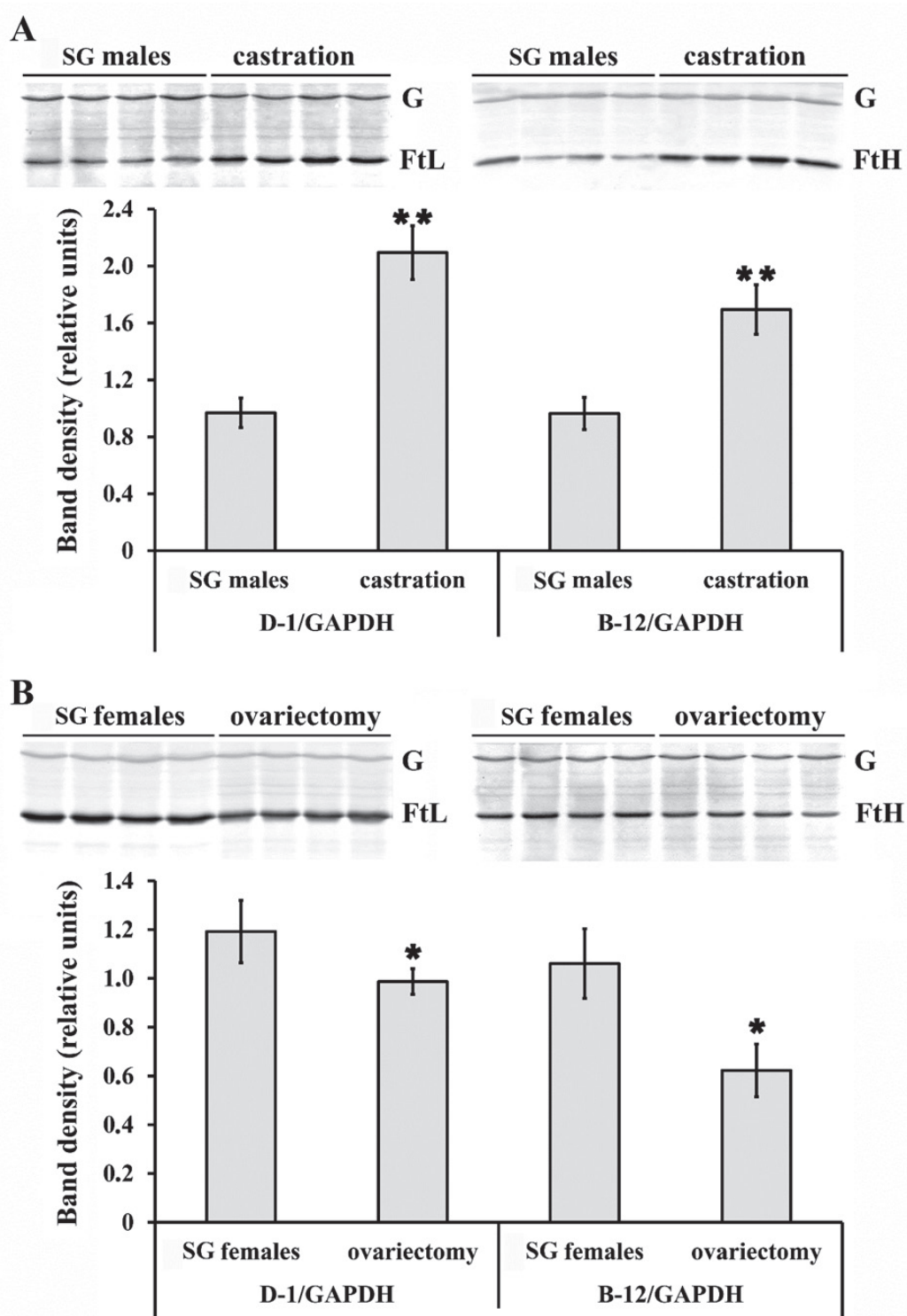


Figure 9 Effect of gonadectomy on both ferritin chain expression in the kidney. Expression of FtL and FtH protein (A, B) in the kidney by western blotting. Each band represents FtL or FtH expression in the tissue of individual animals. Each bar represents mean \pm SEM of band density from four animals per group. Data were analysed with the *t*-test. Additional protein bands are from alpha-tubulin (aT), beta-actin (bA), and GAPDH (G). Ovariectomy statistically decreased the expression of both ferritin chains and castration increased their expression. Statistics: sham-gonadectomised (SG) vs castrated males ** $P < 0.01$ (A); SG vs ovariectomised females * $P < 0.05$ (B)

higher expression of inducible metallothioneins (MT) in some proximal tubules, which may attenuate reactive oxygen species (ROS) or directly sequester iron in organelles (29–33). Also, these vesicles can stay in the cell and form lipofuscin as time goes by (aging pigment of incompletely degraded proteins) (32). Our previous study (21) reports that expelled vesicles to the lumen of proximal tubules through exocytosis may correlate with MT-positive vesicles. It is possible that some reabsorption mechanism takes place in the form of megalin/cubilin scavenger receptors (21), which are present on the apical membrane of the S3 segment of proximal tubules. This is visible in Figure 3 (a and b, bottom).

Interactions between essential and toxic transition metals (TM) and mechanisms that protect or damage the cell/organism have been studied for many years (30). For iron as an endogenous source of ROS, scavenger interactions with ferritin and MT are of particular interest (31–37).

The significance of ferritin is also visible at the molecular level through regulation of iron accumulation and autophagocytosis and recycling of material within the cell (38, 39). Sex differences in autophagy and some diseases call for a revision of current knowledge about the metabolism of iron and other TMs and of implications related to aging, sterile inflammation, and degenerative diseases (40–46). Essential TMs, iron in particular, are involved in all cellular processes, and our study shows that it is important to establish whether sex differences or their absence play an important role in research models and human diseases, as suggested earlier (5, 26, 40–42).

Some novel markers, such as nuclear receptor coactivator 4 (NCOA4) are believed to drive ferritinophagy – autophagic degradation of ferritin that can lead to ferroptosis as regulated cell death independent of apoptosis, with iron lipid oxidation and GSH depletion (38, 39).

One of our aims was to establish the role of aging on ferritin expression. Until now, such an association between aging and iron accumulation in organs or between expressions of the two ferritin chains was studied only individually, like in female liver along with methionine-centred redox cycle changes (11) or in male heart and liver with oral iron chelator that decreased apoptosis protein expression (12), or in the male muscle in relation to protein oxidative damage (47). The last study suggested that accumulated iron and ferritin caused sarcopaenia. However, molecular pathways in aging and the role of ROS-producing iron and both ferritin chains remain elusive (5, 26–28, 30).

Our work contributes to current research with new data on sex and age differences in the expression and distribution of both ferritin chains and provides the background of all physiological processes.

CONCLUSION

Our study returns to the basic questions about the importance of sex, sex hormones, and age in the expression of both ferritin

chains as the main iron storage cell structures by giving new insights into their distribution in the liver and kidney. These insights call for new (patho)physiological and toxicological investigations, which should clarify how the sex and age-dependent relationship between iron and ferritin affects the system, especially in oxidative stress.

Conflicts of interest

None to declare.

Acknowledgements

This study was supported by the Croatian Ministry of Science and Education and the AGEMETAR project funded by the Croatian Science Foundation (grant No. IP-11-2013-1481). We wish to thank the principal investigator Davorka Breljak for organising and assisting with animal tissue sampling and to all colleagues who worked on the AGEMETAR project, Tatjana Orct, Ivana Madunić Vrhovac, and Dean Karaica in particular, to Ivan Sabolić for launching and supervising the project, to Ljiljana Babić for technical support, and to Renata Novak Mirčetić from the Gorea Plus Company for first ferritin antibody tests.

Funding

This work was supported by the Ministry of Science and Education of the Republic of Croatia Program financing for ML and by a grant from the project AGEMETAR funded by the Croatian Science Foundation (grant number: IP-11-2013-1481) for ML and VM.

REFERENCES

1. Plays M, Müller S, Rodriguez R. Chemistry and biology of ferritin. *Metalomics* 2021;13(5):mfab021. doi:10.1093/mtomcs/mfab021
2. Arosio P, Elia L, Poli M. Ferritin, cellular iron storage and regulation. *IUBMB Life* 2017;69:414–22. doi: 10.1002/iub.1621
3. Arosio P, Levi S. Cytosolic and mitochondrial ferritins in the regulation of cellular iron homeostasis and oxidative damage. *Biochim Biophys Acta* 2010;1800:783–92. doi: 10.1016/j.bbagen.2010.02.005
4. Muckenthaler MU, Rivella S, Hentze MW, Galy B. A red carpet for iron metabolism. *Cell* 2017;168:344–61. doi: 10.1016/j.cell.2016.12.034
5. van Swelm RPL, Wetzels JFM, Swinkels DW. The multifaceted role of iron in renal health and disease. *Nat Rev Nephrol* 2020;16:77–98. doi: 10.1038/s41581-019-0197-5
6. Anderson GJ, Frazer DM. Current understanding of iron homeostasis. *Am J Clin Nutr* 2017;106(Suppl 6):1559S–66S. doi: 10.3945/ajcn.117.155804
7. Sangkhue V, Nemeth E. Regulation of the iron homeostatic hormone hepcidin. *Adv Nutr* 2017;8:126–36. doi: 10.3945/an.116.013961
8. Li W, Garringer HJ, Goodwin CB, Richine B, Acton A, Van Duyn N, Muhoberac BB, Irimia-Dominguez J, Chan RJ, Peacock M, Nass R, Ghetti B, Vidal R. Systemic and cerebral iron homeostasis in ferritin knock-out mice. *PLoS One* 2015;10(1):e0117435. doi: 10.1371/journal.pone.0117435

9. Björklid E, Helgeland L. Sex differences in the ferritin content of rat liver. *Biochim Biophys Acta* 1970;221:583–92. doi: 10.1016/0005-2795(70)90230-8
10. Linder MC, Moor JR, Scott LE, Munro HN. Mechanism of sex difference in rat tissue iron stores. *Biochim Biophys Acta* 1973;297:70–80. doi: 10.1016/0304-4165(73)90050-0
11. Bulvik BE, Berenshtein E, Konijn AM, Grinberg L, Vinokur V, Eliashar R, Chevion MM. Aging is an organ-specific process: changes in homeostasis of iron and redox proteins in the rat. *Age* 2012;34:693–704. doi: 10.1007/s11357-011-9268-7
12. Arvapalli RK, Paturi S, Laurino JP, Katta A, Kakarla SK, Gadde MK, Wu M, Rice KM, Walker EM, Wehner P, Blough ER. Deferasirox decreases age-associated iron accumulation in the aging f344xbn rat heart and liver. *Cardiovasc Toxicol* 2010;10:108–16. doi: 10.1007/s12012-010-9068-9
13. Widdowson EM, McCance RA. Sexual differences in the storage and metabolism of iron. *Biochem J* 1948;42:577–81. doi: 10.1042/bj0420577
14. Widdowson EM, McCance RA. The effect of dosage on sexual differences in the iron metabolism of rats. *Biochem J* 1953;53:173–7. doi: 10.1042/bj0530173
15. Kaldor I, Powell M. Studies on intermediary iron metabolism. X. The influence of age and sex on the storage of supplemental dietary iron in the rat. *Aust J Exp Biol Med Sci* 1957;35:123–9. doi: 10.1038/icb.1957.15
16. Kaldor I. Studies on intermediary iron metabolism. XII. Measurement of the iron derived from water soluble and water insoluble non-haem compounds (ferritin and haemosiderin iron) in liver and spleen. *Aust J Exp Biol Med Sci* 1958;36:173–82. doi: 10.1038/icb.1958.19
17. Xu J, Jia Z, Knutson MD, Leeuwenburgh C. Impaired iron status in aging research. *Int J Mol Sci* 2012;13:2368–86. doi: 10.3390/ijms13022368
18. Kong WN, Niu QM, Ge L, Zhang N, Yan SF, Chen WB, Chang YZ, Zhao SE. Sex differences in iron status and hepcidin expression in rats. *Biol Trace Elem Res* 2014;160:258–67. doi: 10.1007/s12011-014-0051-3
19. Directive 2010/63/EU of the European Parliament and of the Council of 22 September 2010 on the protection of animals used for scientific purposes [displayed 22 March 2022]. Available at: <https://eur-lex.europa.eu/eli/dir/2010/63/oj>
20. Ljubojević M, Orct T, Micek V, Karaica D, Jurasović J, Breljak D, Vrhovac Madunić I, Rašić D, Novak Jovanović I, Peraica M, Gerić M, Gajski G, Oguić SK, Rogić D, Nanić L, Rubelj I, Sabolić I. Sex-dependent expression of metallothioneins MT1 and MT2 and concentrations of trace elements in rat liver and kidney tissues: Effect of gonadectomy. *J Trace Elem Med Biol* 2019;53:98–108. doi: 10.1016/j.jtemb.2019.02.010
21. Sabolić I, Škarica M, Ljubojević M, Breljak D, Herak-Kramberger CM, Crljen V, Ljubešić N. Expression and immunolocalization of metallothioneins MT1, MT2 and MT3 in rat nephron. *J Trace Elem Med Biol* 2018;46:62–75. doi: 10.1016/j.jtemb.2017.11.011
22. Orct T, Jurasović J, Micek V, Karaica D, Sabolić I. Macro- and microelements in the rat liver, kidneys, and brain tissues; sex differences and effect of blood removal by perfusion *in vivo*. *J Trace Elem Med Biol* 2017;40:104–11. doi: 10.1016/j.jtemb.2016.12.015
23. Roy A, Al-bataineh MM, Pastor-Soler NM. Collecting duct intercalated cell function and regulation. *Clin J Am Soc Nephrol* 2015;10:305–24. doi: 10.2215/CJN.08880914
24. Broecker KAE, Fuchs MAA, Schrankl J, Lehrmann C, Schley G, Todorov VT, Hugo C, Wagner C, Kurtz A. Prolyl-4-hydroxylases 2 and 3 control erythropoietin production in renin-expressing cells of mouse kidneys. *J Physiol* 2022;600:671–94. doi: 10.1113/JP282615
25. Cohen LA, Gutierrez L, Weiss A, Leichtmann-Bardoogo Y, Zhang DL, Crooks DR, Sougrat R, Morgenstern A, Galy B, Hentze MW, Lazaro FJ, Rouault TA, Meyron-Holtz EG. Serum ferritin is derived primarily from macrophages through a nonclassical secretory pathway. *Blood* 2010;116:1574–84. doi: 10.1182/blood-2009-11-253815
26. McCullough K, Bolisetty S. Ferritins in kidney disease. *Semin Nephrol* 2020;40:160–72. doi: 10.1016/j.semnephrol.2020.01.007
27. Balla J, Balla G, Zarjou A. Ferritin in kidney and vascular related diseases: novel roles for an old player. *Pharmaceuticals (Basel)* 2019;12:96. doi: 10.3390/ph12020096
28. Mahroum N, Alghory A, Kiyak Z, Alwani A, Seida R, Alrais M, Shoenfeld Y. Ferritin - from iron, through inflammation and autoimmunity, to COVID-19. *J Autoimmun* 2022;126:102778. doi: 10.1016/j.jaut.2021.102778
29. Zhang Y, Mikhael M, Xu D, Li Y, Soe-Lin S, Ning B, Li W, Nie G, Zhao Y, Ponka P. Lysosomal proteolysis is the primary degradation pathway for cytosolic ferritin and cytosolic ferritin degradation is necessary for iron exit. *Antioxid Redox Signal* 2010;13:999–1009. doi: 10.1089/ars.2010.3129
30. Valko M, Morris H, Cronin MT. Metals, toxicity and oxidative stress. *Curr Med Chem* 2005;12:1161–208. doi: 10.2174/0929867053764635
31. Baird SK, Kurz T, Brunk UT. Metallothionein protects against oxidative stress-induced lysosomal destabilization. *Biochem J* 2006;394:275–83. doi: 10.1042/BJ20051143
32. Terman A, Kurz T. Lysosomal iron, iron chelation, and cell death. *Antioxid Redox Signal* 2013;18:888–98. doi: 10.1089/ars.2012.4885
33. Pavić M, Turčić P, Ljubojević M. Forgotten partners and function regulators of inducible metallothioneins. *Arh Hig Rada Toksikol* 2019;70:256–64. doi: 10.2478/aiht-2019-70-3317
34. Atrian S, Capdevila M. Metallothionein-protein interactions. *Biomol Concepts* 2013;4:143–60. doi: 10.1515/bmc-2012-0049
35. Orihuela R, Fernández B, Palacios O, Valero E, Atrian S, Watt RK, Dominguez-Vera JM, Capdevila M. Ferritin and metallothionein: dangerous liaisons. *Chem Commun* 2011;47:12155–7. doi: 10.1039/c1cc14819b
36. Silva-Islas CA, Maldonado PD. Canonical and non-canonical mechanisms of Nrf2 activation. *Pharmacol Res* 2018;134:92–9. doi: 10.1016/j.phrs.2018.06.013
37. Pietsch EC, Chan JY, Torti FM, Torti SV. Nrf2 mediates the induction of ferritin H in response to xenobiotics and cancer chemopreventive dithiolethiones. *J Biol Chem* 2003;278:2361–9. doi: 10.1074/jbc.M210664200
38. Stockwell BR, Friedmann Angeli JP, Bayir H, Bush AI, Conrad M, Dixon SJ, Fulda S, Gascón S, Hatzios SK, Kagan VE, Noel K, Jiang X, Linkermann A, Murphy ME, Overholtzer M, Oyagi A, Pagnussat GC, Park J, Ran Q, Rosenfeld CS, Salnikow K, Tang D, Torti FM, Torti SV, Toyokuni S, Woerpel KA, Zhang DD. Ferroptosis: a regulated cell death nexus linking metabolism redox biology, and disease. *Cell* 2017;171:273–85. doi: 10.1016/j.cell.2017.09.021
39. Masaldan S, Clatworthy SAS, Gamell C, Meggyesy PM, Rigopoulos AT, Haupt S, Haupt Y, Denoyer D, Adlard PA, Bush AI, Cater MA. Iron accumulation in senescent cells is coupled with impaired ferritinophagy and inhibition of ferroptosis. *Redox Biol* 2018;14:100–15. doi: 10.1016/j.redox.2017.08.015

40. Lista P, Straface E, Brunelleschi S, Franconi F, Malorni W. On the role of autophagy in human diseases: a sex perspective. *J Cell Mol Med* 2011;15:1443–57. doi: 10.1111/j.1582-4934.2011.01293.x
41. Shapiro JS, Chang HC, Ardehali H. Iron and sex cross paths in the heart. *J Am Heart Assoc* 2017;6(1):e005459. doi: 10.1161/JAHA.116.005459
42. Congdon EE. Sex differences in autophagy contribute to female vulnerability in Alzheimer's disease. *Front Neurosci* 2018;12:372. doi: 10.3389/fnins.2018.00372
43. Andersen RV, Tybjaerg-Hansen A, Appleyard M, Birgens H, Nordestgaard BG. Hemochromatosis mutations in the general population: iron overload progression rate. *Blood* 2004;103:2914–9. doi: 10.1182/blood-2003-10-3564
44. Harrison-Findik DD. Gender-related variations in iron metabolism and liver diseases. *World J Hepatol* 2010;2:302–10. doi: 10.4254/wjh.v2.i8.302
45. Meynard D, Babitt JL, Lin HY. The liver: conductor of systemic iron balance. *Blood* 2014;123:168–76. doi: 10.1182/blood-2013-06-427757
46. Bessone F, Razori MV, Roma MG. Molecular pathways of nonalcoholic fatty liver disease development and progression. *Cell Mol Life Sci* 2019;76:99–128. doi: 10.1007/s00018-018-2947-0
47. Jung SH, DeRuisseau LR, Kavazis AN, DeRuisseau KC. Plantaris muscle of aged rats demonstrates iron accumulation and altered expression of iron regulation proteins. *Exp Physiol* 2008;93:407–14. doi: 10.1113/expphysiol.2007.039453

Ekspresija lakog i teškog lanca feritina u jetri i bubrezima Wistar štakora: spolne razlike, starenje i utjecaj gonadektomije

Feritin je glavni skladišni protein unutarstaničnoga željeza. U korelaciji s ekspresijom feritina, istraživanja na životinjama pokazuju da jetra i bubrezi u ženki nakupljaju više željeza nego u mužjaka. Međutim, dosad se nijedno istraživanje nije bavilo spolnim i dobnim razlikama u ekspresiji lakog (FtL) i teškog (FtH) lanca koji čine feritinski nanokavez. Kako bismo to riješili, oslonili smo se na specifična protutijela i imunokemijske metode za analizu ekspresije obaju feritinskih lanaca u jetri i bubrezima odraslih i starih mužjaka i ženki štakora soja Wistar. Da bismo vidjeli kako spolni hormoni mogu utjecati na ekspresiju feritina, proučavali smo i gonadektomirane odrasle životinje. FtL i FtH bili su izraženiji u odraslih i starih životinja u obama organima u ženki štakora; gonadektomija je povećala ekspresiju u mužjaka, a smanjila je u ženki, što upućuje na to da feritine stimuliraju ženski, a inhibiraju muški steroidni hormoni. Normalna raspodjela feritina u bubrezima i promjena sa starenjem zahtijevaju više pažnje u proučavanju (pato)fizioloških i toksikoloških procesa.

KLJUČNE RIJEČI: epitelne stanice; feritinski nanokavez; hepatociti; imunofluorescencija; interkalirane stanice, metabolizam željeza; *macula densa*; nefron; steroidni hormoni; *western blot*